SSRG International Journal of Mechanical Engineering
ISSN: 2348-8360/ https://doi.org/10.14445/23488360/IJME-V11I10P106

Volume 11 Issue 10, 61-73, October 2024

Original Article

Process Parameter Optimization of Resistance Spot Welding for AMS 4902 Titanium Grade 2 Sheet Metal

Anishkumar H. Gandhi[1], Prashant Hasmukhray Solanki[2]

[1]*RM LEGAL, Company Secretary, Patent and Trademark Attorneys, Gujarat, India.*
[2]*Gujarat Technological University, Gujarat, India.*
[2]*Production Engineering, Lukhdhirji Engineering College, Gujarat, India.*

[1]*Corresponding Author : anishgandhi2002@yahoo.co.in*

Received: 07 August 2024 Revised: 09 September 2024 Accepted: 07 October2024 Published: 30 October 2024

Abstract - *One method frequently used in the aerospace industry to join sheet metal is resistance spot welding or RSW. This RSW technique works especially well for lap joining thin titanium sheets when joint access is restricted. However, overheating and insufficient nugget formation during RSW makes it difficult to obtain strong welds on pure titanium sheets. Therefore, in order to achieve optimal tensile strength during the RSW process, the parameters such as electrode force, weld current, and weld time were optimized in this study. The experiments were conducted on 1 mm thick AMS 4902 grade 2 titanium metal sheets as per the full factorial Design of the Experiment (DoE). Then, those experiments were verified for defect-free welding with the help of Non-Destructive Testing (NDT) methods. Later, the microstructural analyses showed adequate grain structures on the nugget region. Ultimately, the welding parameters were fine-tuned to align with the goal of maximizing tensile load. This means that the best RSW parameter for achieving a maximum tensile load of 8397.04N at 0.9989 desirability is 10kA current, 40 cycle time, and 6000N electrode force. The optimized solution was confirmed through experimentation, with only a 0.04% margin of error detected. Hence, the proposed DoE and optimization technique may be helpful for aerospace industries while optimizing RSW parameters for a desired tensile load.*

Keywords - *Resistance spot welding, Dye penetration, Tensile load, Titanium, Full factorial design.*

1. Introduction

Titanium and its alloys have unique mechanical and physical properties and are found in major applications in different industrial sectors [1]. These materials have been widely utilized for a large number of applications in the industry due to their excellent corrosion behaviour [2], lower thermal conductivity [3], less specific gravity [4], low density [5] as well as exert relatively high melting temperature [6], which makes them more feasible for aerospace applications [7]. Due to their high strength-to-weight ratio, their applications are also extended to the medical industry, vehicle manufacturing industries, and chemical engineering [5]. Particularly in aircraft parts such as engine turbine blades [8], landing gears [9], engine parts [10], etc., titanium and its alloy parts are mostly utilized. Nonetheless, the process of welding titanium and its alloys is intricate due to the high temperature-induced chemical reactivity of titanium metal. While conducting the weld operation, titanium alloys highly react with the oxygen and nitrogen from the surrounding environment [11, 12]. In addition, titanium is a high-reactivity metal and must be welded under a controlled atmosphere with inert gas shielding to prevent oxidation and maintain weld integrity. However, this makes the welding process even more challenging in Resistance Spot Welding (RSW), where the requirement of a constant and clean environment is particularly important to create strong joints.

Since titanium alloys show only reasonable weldability characteristics, the joint properties are greatly influenced by the welding processes [13]. Titanium alloys have been welded using a variety of welding processes, including Plasma arc welding [14], tungsten inert gas welding [15], laser welding [16], etc. However, they exerted certain limitations regarding economic and physical characteristics such as high heat-affected zones, formation of residual stress, and high-cost equipment [17, 18]. The RSW is a widely used welding technology that mostly applies to attaching metal sheets. It offers several economical and implementation benefits, including great efficiency, cheap cost, simple operation, and minimal noise [19]. RSW is also flexible enough to join complex geometries and configurations, which are required for modern manufacturing processes of rapid production and high precision. Automation and robotics have also brought advancements that further expand the utility of RSW in virtually all industries in high-volume production. Nowadays, its applications are far more widened in sectors such as vehicle

manufacturing, production of electronic devices, rail vehicle parts, precision instruments, aircraft, etc., [20]. In the RSW technique, two electrodes are used to press the overlapped areas of two metal plates and are subjected to a brief, extremely high welding current. According to Joule's law, when the welding current is cut off, the interface's heat is melted and forms a solid junction [21].

RSW is a highly advantageous method for generating large quantities of spot welds due to its speed, flexibility, dependability, and automation. Additionally, a less molten pool obtained through a short welding cycle helps avoid microstructural alterations and damages, which cause lower weld strength [22]. The resistance spot welding process produced ultrafine-grained/nanostructured titanium alloy joints [23]. The RSW analysis is extensively available for joining similar and dissimilar metals [24, 25]. Kumar et al. [26] joined thin sheets of Ti-6Al-4V alloy through the RSW process and analyzed the effect of weld cycle time on the mechanical characteristics of the joint.

On the other hand, Klimenov et al. [23] achieved a finely dispersed martensitic structure of the same alloy joints using the RSW, which helped in improving the microhardness of the welding. Sharma et al. [27] also improved the morphological characteristics and structural properties of RSW-joined Al6063 sheets. Zhong et al. [28] evaluated the effect of electrode cap size and welding current over the nugget characteristics of TL091 alloy joints, which are welded using the RSW process. The outcomes of the study stated that the geometry of the electrode cap affects the bonding between the alloy and the electrode. However, Mansor et al. [29] analyzed the effects of joining stainless steel with titanium alloy using RSW over the microstructural and mechanical properties of the joint. Also, Bamberg et al. [30] studied the cladding of AW-6111 alloy with AW-4040 alloy using the RSW technique and established a uniform welding lobe placement for efficient welding. Additionally, electrode erosion behaviour is analyzed, resulting in irregular nuggets at different spots for the same weld parameters.

Due to its intricacy, the process becomes extremely non-linear, and uncertainties continue to exist even when constant welding parameters are used, resulting in differences in the ultimate quality of the weld [31]. In RSW, the welded nugget size and microstructure of the melted region at the plate interface are highly influenced by various variables, such as base metal characteristics, surface conditions, and welding parameters. These factors ultimately impact the mechanical behaviour of the welds, which is mostly the interfacial shear strength of the joint [27]. The hardness of the welded joint was significantly lowered due to an increase in welding current and duration, which also brought about a coarsening of the weld nugget's grain structure and heat-affected zone [32]. Butsykin et al. [33] investigated the controlling parameters of the RSW process while joining Ti-2Al-1Mn alloy sheets. The author also stated that the preheating of the joint using a preliminary current cycle positively impacted the mechanical behaviour of the joints.

Nowadays, the optimization of parameters and their responses also helps in improving the RSW process by analyzing the influential parameters of the process. Prashanthkumar et al. [34] conducted a thermal analysis on closed rolled and annealed metallic sheets to determine influential parameters on the RSW. The author compared the experimental and simulation results and obtained the optimal current requirement and spotting time for the RSW of the sheets. Cao et al. [35] optimized the RSW process of aluminium silicate-coated boron steel sheets using RSM and genetic algorithm. The welding current, applied force, and cycle time are the considered parameters for enhancing the weld nugget with better shear strength. The accuracy of the shear strength and nugget diameter predictions are 97.62% and 98.04%, respectively. The aluminium silicate coating also helped effectively bond the sheets during the RSW process. Rawal et al. [36] used Taguchi L27 orthogonal array integrated with grey relational analysis to optimize the RSW process of SS304 steel. They enhanced the input parameters such as welding current, electrode pressure, and weld cycle. This method showed a 10% improvement in the nugget dimension and the tensile strength of the weld. Wan et al. [37] optimized RSW through principal component analysis and genetic algorithm for welding the TC2 titanium alloy sheets. The optimized RSW process is more energy efficient and less costly to operate than traditional welding methods, thus making it more economically viable. It also means that lower energy consumption helps reduce carbon emissions, creating another potential environmental touchstone. This study is practical in advancing sustainable manufacturing practices because of these factors.

RSW is an important joining technique because it is consistent and effective. However, weld quality in materials such as AMS 4902 Ti Grade 2 is difficult to achieve optimally due to the material's unique characteristics and sensitivity to welding parameters. The main issue is understanding how different process parameters (welding current, electrode force and welding time) affect weld quality. While existing studies have examined individual parameters or different materials, the optimization of comprehensive AMS 4902 Titanium Grade 2 has not been studied.

Most existing studies deal with the effects of different welding parameters isolated or other Ti grades or alloys without providing a systematic optimization approach for AMS 4902 Titanium Grade 2. The effects of welding parameters in producing optimal mechanical strength and defect-free welds for this material have not been investigated. Furthermore, there is limited attention to integrating Non-Destructive Testing (NDT) to verify weld integrity in these studies.

This study fills this gap by systematically analyzing the most important RSW parameters, such as welding current, electrode force, and AMS 4902 Titanium Grade 2 cycle time. This research provides a complete understanding of achieving optimal weld quality for aerospace applications using Design of Experiments (DoE) and validating results with microstructural analysis and NDT methods. This novel integrated approach focuses on Grade 2 titanium and provides an understanding of optimizing RSW for high-performance structural parts.

The proposed study is organized as an introduction section (section 1) that contains an overview and related studies on the RSW and titanium metals, followed by materials and methods in Section 2, which discusses the selection of materials and parameters for designing the experimentation. Section 3 explains the procedures adapted for the experimentation. Section 4 analyses the DoE through ANOVA. The outcomes from the experimentations are discussed in Section 5. Finally, the summarized findings from the experimental outcomes and the future scope of the present study are presented in Section 6.

1.1. Glossary of Terms

Term	Definition
Resistance Spot Welding (RSW)	RSW is a welding process that joins two or more metal sheets by applying heat and pressure through electric resistance.
AMS 4902 Grade 2 Titanium	A specification for commercially pure titanium sheets with a minimum purity of 99.6%, which is commonly used in aerospace applications.
Design of Experiments (DoE)	DoE is a statistical method for planning, conducting, analyzing and interpreting controlled tests to evaluate the factors influencing outcomes.
ANOVA (Analysis of Variance)	ANOVA is a statistical method used to determine if there are significant differences between the means of three or more groups.
Electrode Force	The amount of pressure electrodes apply to hold the metal sheets together during the welding process.
Cycle Time	The duration of the welding process is from the beginning of the current flow until it is stopped.
Welding Cycle	The duration of the welding process is measured in cycles, which include the time for heating, cooling, and any hold time.
Welding Current	The electric current applied during the welding process is important for generating the heat needed to melt materials being joined.
Tensile Loading Capacity	The maximum load that welded joints withstand when subjected to tensile stress.
Nugget	The melted and solidified zone formed during the welding process, which is the actual weld area.
Yield Strength	The stress at which material initiates to deform plastically.

Table 1. Chemical elements and mechanical properties of AMS 4902 Gr 2 Ti sheet

Chemical Elements						
Elements	**Fe**	**O**	**N**	**C**	**H**	**Ti**
Wt. %	0.030	0.070	0.014	0.049	0.004	Balance
Mechanical Properties						
Properties at 20℃	**Tensile Strength (MPa)**		**Yield Strength (MPa)**	**Hardness (HRD)**	**% Elongation**	
Value	491		317	58	39	

2. Materials and Methods

2.1. Material Selection and Properties

The commercially available 1mm thick grade 2 pure titanium sheets within Aerospace Material Specification (AMS) system 4902 (AMS 4902 Gr 2 Ti) were used as a substrate material for RSW in this study. This AMS 4902 Gr 2 Ti material consists of 99.6% pure Titanium and a very small amount of strengthening elements, as given in Table 1 (as per the material supplier test report). Since the selected AMS 4902 Gr 2 Ti was mainly used as a building material for aerospace structural components such as airframe skins, brackets, ductwork, etc., lap joining is a common practice. The RSW lap joining experiments are conducted on AMS 4902 Gr 2 Ti sheets in this study. The sheets were welded with the help of a Copper-Chromium electrode rod of 5mm in diameter.

2.2. Parametric Selection

The RSW consists of many process parameters such as current, electrode force, material thickness, electrode material, etc. Thus, identifying optimal RSW parameters for the

selected AMS 4902 Gr 2 Ti metal sheet is a consuming and almost impossible task with limited availability of resources. Therefore, based on the literature [35], the welding current, welding cycle, and electrode force were identified as the most influencing RSW process parameters for this study. Afterwards, trial and error experiments were conducted to identify the study range for each parameter. As a result, welding current was identified as the topmost effective RSW parameter for the AMS 4902 Gr 2 Ti metal sheet. Increasing the weld current beyond 10kA, a dent failure has occurred on top of the weld surface, as shown in Figure 1. Thus, the maximum weld current and its respective other two parameters were restricted up to 10kA (current), 6000N (force), and 40 cycles (weld time).

Similarly, no significant joint was observed for a weld current of less than 8kA. Therefore, the 8kA was taken as the minimum welding current according to Table 2. Welding current and experimental trials also inform the selection of the other two RSW parameters. After identifying the RSW process parameters, the weld quality was determined based on tensile strength, micro-hardness, microscopic evaluations, and certain NDTs, as mentioned in the experimental procedure.

Fig. 1 Dent formed during trial and error experiments

Table 2. RSW process parameters and their range

Parameters	Unit	Low-Level	Mid-Level	High-Level
Welding Current	kA	8	9	10
Welding Time	cycle	20	30	40
Electrode Force	N	2000	4000	6000

2.3. Design of Experiments

The welding experiments are performed based on a 3x3 full factorial DoE approach, which includes all possible combinations of selected study parameter levels. Therefore, the optimization model can provide better and more accurate results when compared to other available DoEs, such as Taguchi's orthogonal array, Box Behnken, Central Composite, etc. [38]. Moreover, the study material is mostly used in sensitive applications like aircraft skins and chemical reactor vessels, where safety is a major concern [18]. The commercially available Minitab Statistical Software version 21.4.1 is used for creating a 3-factor, 3-level full factorial-based DoE for this study. In this study, the desirability function optimization technique is well suited to the choice of an optimization technique as it allows for simultaneous optimization of multiple response variables, thereby ensuring the best trade-offs. The desirability function is compared with other methods, such as response surface methodology, which is easier to use in critical applications to achieve the desired quality with conflicting objectives. Its ability to handle different types of responses adds to its applicability to this study. Further, the RSW experiments are conducted on prepared AMS 4902 Gr 2 Ti metal sheets, and their respective tensile loading capability is evaluated, as shown in Table 3.

Table 3. RSW experiments based on the 3x3 full factorial DoE method

Run Order	Welding Current (kA)	Welding Time (Cycle)	Electrode Force (N)	Tensile Load (N)
1	10	20	6000	8020
2	9	20	4000	6740
3	9	30	2000	7380
4	10	40	6000	8400
5	10	30	6000	8040
6	10	20	4000	8080
7	9	40	2000	8280
8	8	40	6000	6800
9	9	40	4000	7100
10	10	30	2000	7980
11	8	40	2000	5680
12	10	40	4000	8260
13	8	30	2000	6200
14	9	20	2000	7340
15	9	40	6000	8200
16	9	20	6000	7600
17	8	30	6000	6780
18	8	20	4000	5600
19	10	30	4000	7940
20	8	40	4000	6880
21	10	20	2000	7320
22	9	30	6000	8000
23	9	30	4000	6660
24	8	20	2000	5880
25	8	30	4000	6840
26	10	40	2000	8120
27	8	20	6000	6000

3. Experimental Procedure

After preparing the DoE, the welding experiments are performed using the RE-20 model Pneumatic Spot Welding Machine, which has a 20kVA power rating at 50% duty cycle and needs 380/440V 2-phase input supply as specified in Table 4. The typical lab joints were made on 100x30x1mm

specimens with 30mm overlapping, as explained in Figure 2. Since the welding experiments are conducted based on the proposed DoE as per Table 3, 54 specimens are sliced from the purchased 1000x1250x1mm AMS 4902 Gr 2 Ti sheet for fabricating 27 different tensile test specimens, as shown in Figure 3. Before starting the RSW, the sliced welding specimens were cleaned with the help of an acetone solution to remove dust and other foreign contaminations, as mentioned in existing literature [39]. The welding experiments are assumed at a 95% confidence level because there may be uncertainties possible due to environmental conditions and the experience of a human operator. Random experimental runs were repeated 5 more times to ensure this scenario, and acceptable tensile strength deviations (5-6%) were noticed. Thus, the assumed 95% confidence level was ensured in this study.

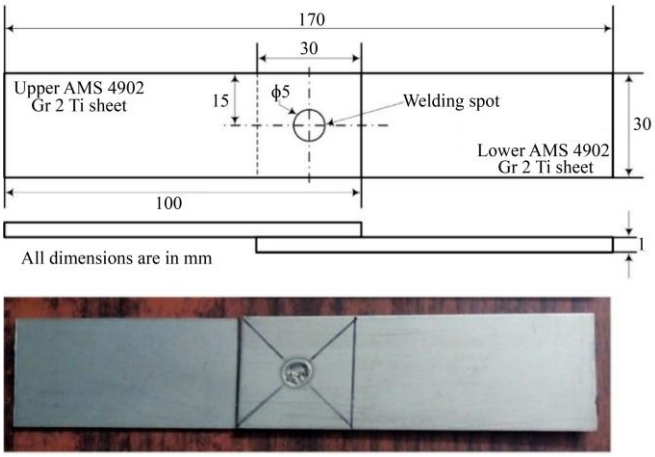

Fig. 2 Dimensional specification of RSW specimens

Table 4. Specifications of the RSW machine

Mechanism / Model	Pneumatic / RE-20
Rated Power	20kVA at 50% Duty Cycle
Phase / Input Supply	Two / 380/440 Volts
Throat Depth	50cm
Maximum Electrode Force	450 at 6kg/cm^2
Maximum Upper Electrode Stroke	50mm
Maximum Available Short Circuit Current	10000A

Moreover, two different NDTs, a dye penetration test and an ultrasonic test, were conducted to analyze the weld quality. For the dye penetration test, the welded samples are first cleaned with Isopropyl Alcohol solvent, then rinsed with distilled water and dried for applying penetrant on its surface. The bright red dye was used as a penetrant for this study. After 10 minutes of dwell time, the excess dye was wiped using a cotton cloth. Then, the developer was applied on the same surface, allowing it to react with the dye for half an hour. Finally, a visual inspection was done to identify any dye bleeding from the weld surface to specify weld quality [40]. Besides, to inspect internal weld defects, another NDT called Ultrasonic testing was conducted according to the American Society of Mechanical Engineers (ASME) standard section VIII division 1. The specifications of the ultrasonic transducer used and testing details are given in Table 5. This NDT method was already verified and suggested by an existing author, Deepak et al. [41], where the weld quality of butt joints was studied. Hence, these NDT methods are significant for identifying the weld defects on resistance spot welded AMS 4902 Gr 2 Ti sheet in this study.

Fig. 3 Resistance spot welded samples for further evaluations

Table 5. Specifications and ultrasonic testing details

Test Material	ASM 4902 Gr 2 Ti sheet
Test Equipment	Einstein – II TFT Ultrasonic Flaw Detector
Test Standard	ASME section VIII, division 1, appendix 12
Testing Method	Pulse Echo method
Surface Condition	Smooth and clean
Material Thickness	1mm
Number of Specimens	27
Study Zone	Weld spot (Nuggets)
Probe Type	T/R
Study Range and Frequency	0-20mm and 4MHz
Reference /Scanning Sound	54dB / 60dB

After verifying the weld quality through such NDT methods, the welded specimens underwent certain destructive testing to evaluate weld strength as follows. Initially, the tensile loading capacity of each sample is examined using a Universal Tensile Machine (UTM), as shown in Figure 4. The tensile tests were conducted at atmospheric pressure and room

temperature with 5mm/min loading conditions. The maximum tensile loading capacity of the UTM machine used was 50kN. Based on tensile results, 3 specimens that show low (exp no. 18), intermediate (exp no. 14), and high (exp no. 4) tensile capacity are selected for further evaluation of microstructural properties. Thus, those 3 selected experiments were repeated, and samples were collected for microscopic and micro-hardness studies. To improve their surface details, the microscopic samples are first etched with a chemical solution containing 15% HCl, 5% HF, and 80% water. Similarly, the micro-hardness of the samples is tested using a Vickers Hardness testing machine, as shown in Figure 5. The samples used for microscopic and micro-hardness studies are shown in Figure 6.

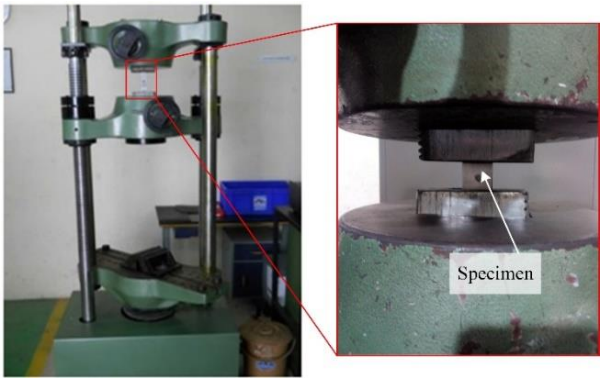

Fig. 4 Universal tensile testing machine

Fig. 5 Micro-hardness testing machine

4. Analysis of Variance (ANOVA)

The significance of each welding parameter on the tensile load carrying capacity of ASM 4902 Gr 2 Ti sheet is studied using the Analysis of Variance (ANOVA) approach as given in Table 6. According to ANOVA results, it is inferred that the proposed DoE model is significant for optimization since the P-value was less than 0.05 [42]. Also, welding current and time parameters are identified as significant process parameters on tensile load, with 70.62% and 7.59% contributions, respectively.

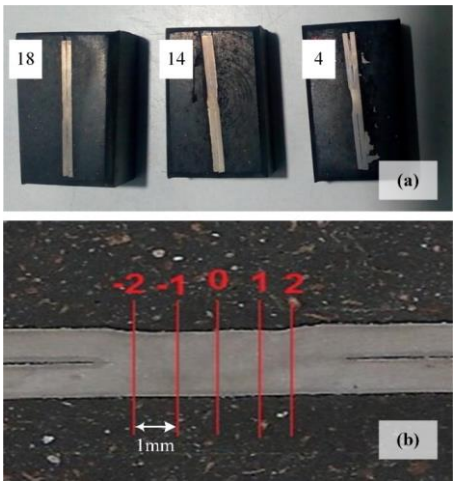

Fig. 6 Test samples for (a) microscopic study, and (b) micro-hardness study.

However, the electrode force does not significantly impact tensile load, and its contribution towards the change in load-carrying capacity of the proposed material is very similar to that of welding time, as indicated by ANOVA results. The ANOVA results clearly illustrate the effect of welding parameters on tensile load. The high F value for welding current (42.39), in comparison to relatively low values for other parameters, suggests that it dominates the influence on tensile strength. The large effect of welding current and time further suggests that there is potential for performance improvement by optimizing these parameters. Additional statistical validation can increase the robustness of the findings, which makes them reliable in other experimental conditions.

Table 6. ANOVA results for tensile load

Source	DF	Adj SS	Adj MS	F-Value	P-Value	Contribution
Model	6	16481333	2746889	16.67	0.000	-
Linear	6	16481333	2746889	16.67	0.000	-
Welding Current (kA)	2	13965896	6982948	42.39	0.000	70.62%
Welding Time (cycle)	2	1501007	750504	4.56	0.023	7.59%
Electrode Force (N)	2	1014430	507215	3.08	0.068	5.13%
Error	20	3294696	164735	-	-	16.66%
Total	26	-	-	-	-	100.00%
DF- Degrees of Freedom; Adj SS - Adjusted Sum of Squares; Adj MS - Adjusted Mean Square						

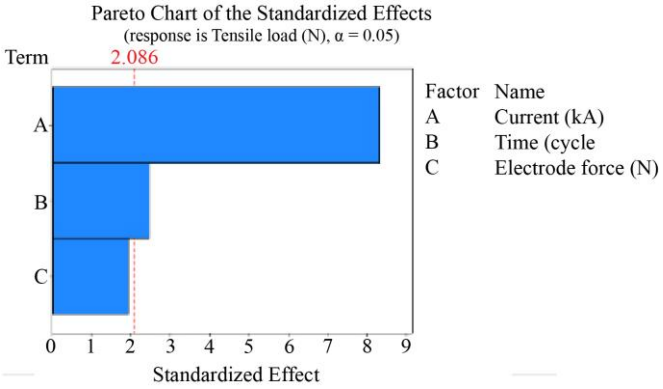

Fig. 7 Pareto chart for tensile load

The significance of each input RSW parameter on the tensile loading capacity of ASM 4902 Gr 2 Ti is confirmed with the Pareto chart, as shown in Figure 7. Since the bar graphs of both welding current and welding time exceed Lenth's Pseudo threshold value of 2.086, these two process parameters significantly impacted tensile load. This statement was also confirmed by an existing research article published by Khammass Hussein [43].

5. Result and Discussion

5.1. Assessment of Weld Quality

5.1.1. Ultrasonic Test

The integrity of the RSW can be ensured through non-destructive type ultrasonic testing. It can investigate the presence of cracks or voids and other non-noticeable weld defects upon ordinary visual inspection [44]. The ultrasonic echo obtained for the non-defective weld specimen is shown in Figure 8. A similar pattern is obtained for all 27 specimens considered for the study. Therefore, it confirms that the weld is free of defects such as voids and cracks. The uniform grain structure around the weld nuggets may helped in producing better ultrasonic attenuation. Since homogeneous melting is obtained through the range of welding parameters, the chances of obtaining lower ultrasonic attenuation are reduced. The better attenuation coefficient means a higher hardness range. Echoes among principal echoes are also noticed due to the difference in the beam and nugget dimensions [45].

Fig. 8 Ultrasonic testing of weld

5.1.2. Dye Penetration Test

The dye penetration test has been considered an effective way to analyze the surface quality of welded samples [46]. The dye penetrant test can detect cold shuts, porosity, lack of fusion, and cracks in the welded specimens. In order to obtain precise outcomes, a set of surface clean-up processes is conducted before subjecting the specimens to a dye penetration test. The clean-up is executed through grinding welded samples and a visual examination, ensuring the dryness and absence of dirt, grease, weld spatter remains, and oil remnants that could hide surface defects and openings. The RSW parametric influence on the weld quality is inspected under appropriate lighting and good eyesight conditions. Visual inspection is a cost-efficient method for evaluating the weld quality, which requires only a few pieces of equipment to inspect the weld quality.

During the visual inspection, the lighting condition was maintained at 550 lux [47]. Figure 9 shows the spot welded specimens infused with the developer subjected to visual inspections. The discontinuity and defects in the weld are evaluated through these developer-infused specimens. If any dye bleeding in the developer-applied region occurs, that specimen is considered fault one. Otherwise, the welds are proper and in good condition. As per the standard investigation, no defects or imperfections are observed in any of the 27 specimens. Furthermore, the other side of the specimens was subjected to the dye penetration inspection, providing similar observations. Therefore, all 27 samples passed the dye penetration test, proving that the considered weld parameter range is effective for the RSW of AMS 4902 Gr-2 material.

Fig. 9 Dye penetrant test samples

5.2. Tensile Results

Table 3 shows the maximum tensile load (8400N) carrying capacity from the welded specimen at experiment number 4, where the welding current, welding time, and electrode force, respectively, are at 10kA, 40 cycles, and 6000N. This extreme tensile load is mainly due to the high rate of metal diffusion and bonding caused by increased current and electrode force.

Figure 10 illustrates that the tensile load capacity of welded samples tends to increase as all three RSW parameters are increased. More precisely, when the welding current was raised from 8kA to 9kA, the tensile load was significantly increased from 6295N to 7478N. Similarly, there was a definite increase in tensile loading capacity from 6953N to 7524N while increasing welding time from 20 to 40 cycles.

In contrast, no significant improvement was observed from the tensile testing specimens prepared at 2000 and 4000-newton electrode pressure. The insufficient binding force resulting from an electrode force of up to 4000N may explain this phenomenon. However, a substantial enhancement in tensile load, reaching 7540N, is observed when the electrode force is increased to 6000N.

The significant impact of two parameters on tensile load was analyzed through colour contour plots, as shown in Figure 11. From Figure 11(a), increasing welding time at low and medium levels of welding current does not improve the tensile load of the specimen. This indicates the upper hand of welding current while improving tensile load over welding time.

Figure 11(b) shows a maximum tensile load of more than 8000N at an electrode force of approximately 5500N and welding current above 9.5kA. However, the electrode force and welding time have very little impact on tensile load, as shown in Figure 11(c). Hence, the maximum tensile load achieved at these conditions is in the range of 7500-8000N only.

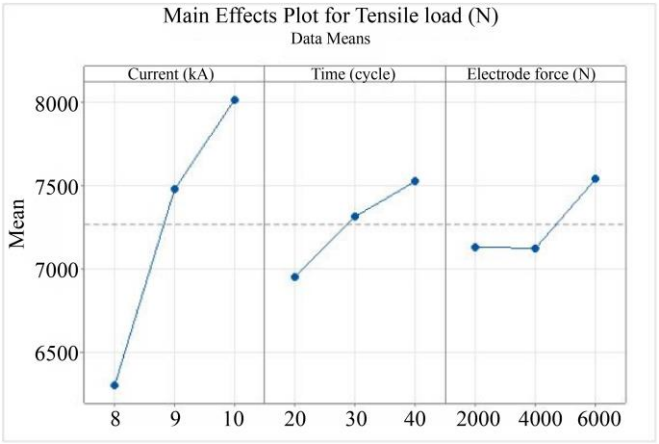

Fig. 10 Main effect plot for tensile load

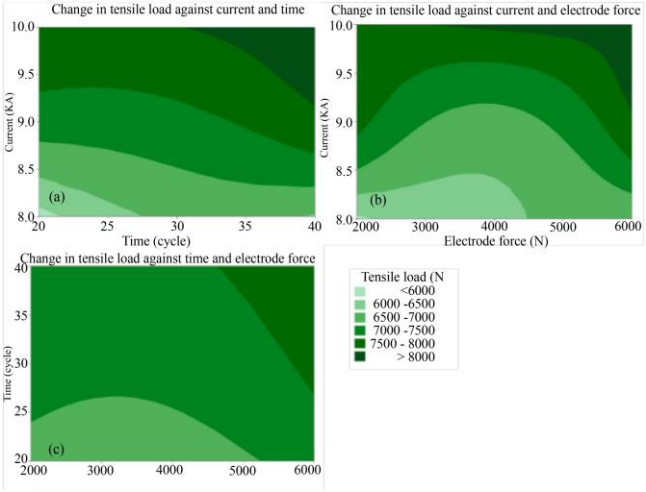

Fig. 11 Contour plots of tensile load (a) Welding time vs welding current, (b) Electrode force vs welding current, and (c) Electrode force vs welding time.

5.3. Microstructural Analysis

The microstructure of RSW joined pure titanium alloy specimens with maximum, intermediate, and minimum tensile strength are depicted in Figure 12(a), (b), and (c), respectively. Scanning Electron Microscopy (SEM) was used for the microstructural analyses. After the tensile test, the specimen that produced the highest, intermediate, and minimum values is chosen, and it is refabricated for microstructural examination using the same welding conditions and surroundings. The specimen has a few needle-like features and fine alpha-structured grains with maximum tensile strength. The alpha-structured grains commonly occur due to the annealing of titanium during the welding process. Kaya et al. [39] also reported that annealing of the titanium produces fine equiaxed alpha grains at 600–700°C range. Meanwhile, the needle structure occurs due to the formation of a martensitic phase in the titanium [48]. However, twinning of the structures is not seen in the specimen, which ensures that applied electrode pressure is efficient because twinning in titanium metals is caused by deformation force applied over the titanium specimen [49].

The specimen that exerted intermediate tensile strength showed a similar structure to the maximum tensile strength specimen. There is just a slight increase in needle structure, which could be the consequence of lower electrode pressure and welding current. However, the strength is maintained at an intermediate level and is not significantly impacted by this structural variation. In the meantime, there is more needle structure in the minimal tensile strength specimen, which could cause the decreased tensile strength. The increased needle structure in this specimen is caused by a reduced welding cycle and welding current. Nevertheless, none of the specimens under consideration exhibit any signs of porosity or cracks. Also, only common and justifiable issues are observed in the microstructure images, which proves that the considered parametric ranges are feasible for the RSW of titanium grade-2 aero craft materials.

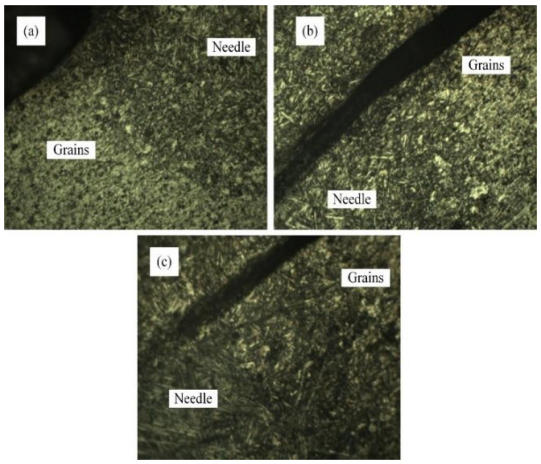

Fig. 12 Microstructure of RSW joined specimens with (a) 5600N (minimum) tensile load, (b) 7340N (intermediate) tensile load, and (c) 8400N (maximum) tensile strength.

5.4. Microhardness

The distribution of hardness around the weld nuggets in the RSW joined specimens with maximum, intermediate, and minimum tensile strength specimens is compared in the graph shown in Figure 13. From the graph, an uneven distribution of hardness around the weld nugget is observed for the minimum tensile strength specimen.

This uneven distribution in the nugget may be the reason for the joint's tensile strength reduction. The reduced welding cycle resulted in this uneven distribution of the hardness in the RSW-joined specimen with minimum tensile strength [39].

However, an almost even hardness distribution is observed for both of the remaining specimens with maximum and intermediate tensile strength.

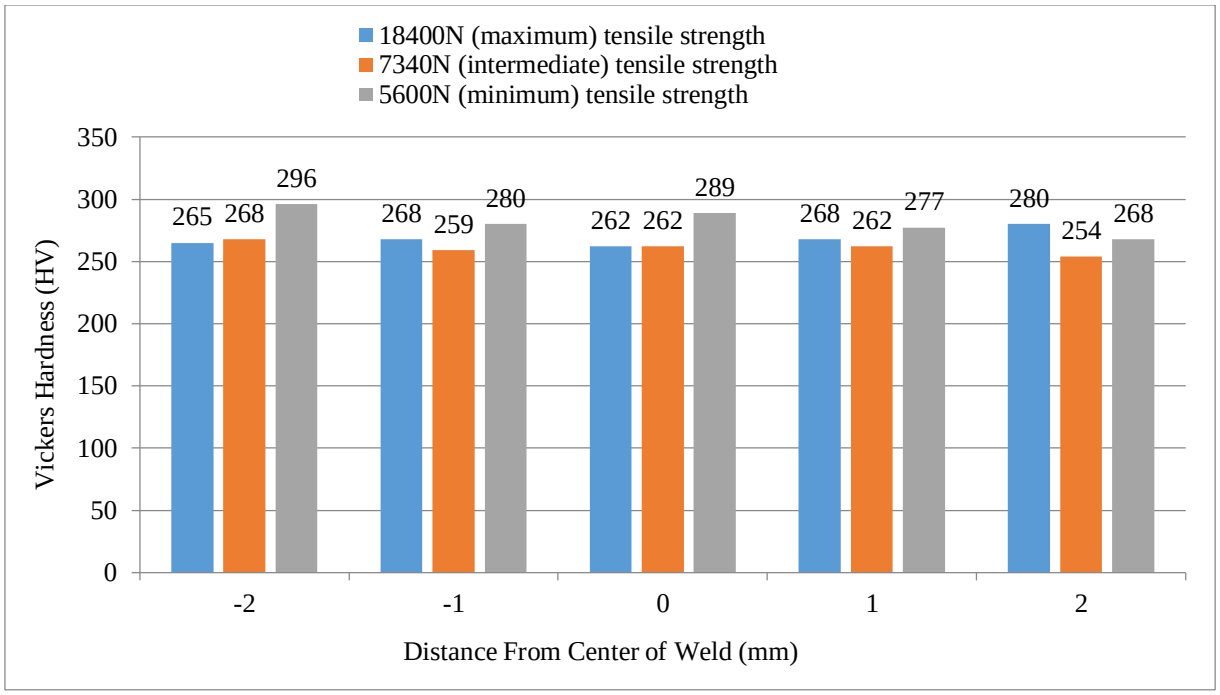

Fig. 13 Microhardness of the welded specimens with 5600N (minimum), 7340N (intermediate), and 8400N (maximum) tensile strength

5.5. Optimal Welding Parameters

This study aims to optimize RSW parameters to achieve the maximum tensile load-carrying capacity of AMS 4902 Gr 2 Ti. The response optimization was done with the help of the proposed full factorial DoE to achieve this output. The maximum goal was selected for the output response tensile load with the highest importance and weight value of 1.

Table 7 displays the top three ideal solutions that the DoE model yielded in accordance with the stated objectives. The AMS 4902 Gr 2 Ti sheet, which is 1 mm thick, can have an ideal tensile load capacity of 8397.04N when it is welded at 10kA current, 40 cycle duration, and 6000N of electrode force, according to the proposed DoE and ideal parameters. The composite desirability reached, which is 0.998942, demonstrates the effectiveness of the optimal solution. This value is extremely close to 1, similar to the findings of Rajalingam et al. [50].

Nonetheless, confirmatory tests assess the top 3 optimal alternatives, resulting in a maximum error of 1.43% for the third solution and only 0.04% for the chosen best solution. Thus, based on the results of this study, this approach may be useful for maximizing RSW process parameters for aerospace-grade pure titanium and its alloy sheets.

Table 7. Top 3 optimal solutions obtained for tensile load

Solution	Welding Current (kA)	Welding Time (cycle)	Electrode Force (N)	Tensile Load (N)	Composite Desirability	Actual Tensile Load (N)	Error (%)	Remark
1	10	40	6000	8397.04	0.998942	8400	0.04	Selected
2	10	40	4000	8365.93	0.987831	8260	1.28	Acceptable
3	9	40	6000	8317.04	0.970370	8200	1.43	Acceptable

5.6. Comparison of Proposed Study with Previous Studies

Table 8 presents the comparison of the proposed study with previous studies. Compared to other studies, this study focused on AMS 4902 Grade 2 titanium, which is important in aerospace applications and enhances its relevance to industry standards. The use of FFD allows for a comprehensive analysis of the effects of multiple parameters on welding quality, which provides a systematic approach that is less considered in previous studies. Verifying weld quality through non-destructive testing methods highlights the consistency of results, confirming that the welds are defect-free. This is an essential aspect of aerospace applications. The study achieved tensile load with only 0.04% error at 10kA current, 40 cycle time and 6000N electrode force optimal parameter, highlighting the accuracy of the proposed study's methodology and findings.

Table 8. Comparison of the proposed study with previous studies

Aspect	Key Parameters	Material	Methodology	Findings
Proposed Study (AMS 4902 Titanium Grade 2)	Electrode force, weld current, weld time	AMS 4902 Titanium Grade 2 (1 mm thick)	Full factorial Design of Experiment (DoE) and NDT methods	Optimal parameters: 10 kA current, 40 cycles, 6000 N force; max tensile load: 8397.04 N
Zhao et al. [51]	Weld current, weld time	Titanium alloy sheets	Entropy weight and regression analysis	Identified welding current as the most significant factor
Zhao et al. [52]	Welding current, voltage	TC2 Titanium alloy (0.4 mm thick)	Regression models and ANN	Developed robust regression models for nugget diameter
Mezher et al. [53]	Welding current, pressure, time	Titanium Grade 2 sheets (1 mm and different thicknesses)	DOE with ANN	Maximum shear force and HAZ hardness improvement
Uppada et al. [54]	-	General	Artificial immune algorithm	Established optimized parameters for load capacity
Bozkurt et al. [55]	Electrode force, weld current, time	Ti6Al4V (α-β titanium alloy)	Taguchi L9 orthogonal design	Highest strength obtained under certain conditions
Taufiqurrahman et al. [56]	Weld current, electrode force	SS316L/Ti6Al4V	Experimental analysis with various parameters	Examined phase transformations and intermetallic compo

6. Conclusion

Thus, this study analyzed the relationship between lap-jointed AMS Gr 2 Ti sheet metal's tensile loading capacity and the most influencing RSW parameters through a series of controlled experiments. The valuable findings of this study are summarized as follows,

- Dent failures in welded specimens were observed during preliminary experiments, increasing weld current by more than 10kA. Hence, it is recommended to maintain a welding current below 11kA when performing RSW on 1mm thick AMS 4902 titanium grade 2 sheets.
- The ANOVA and Pareto results verified that welding current and welding time impacted the tensile load carrying capacity of lap-jointed AMS 4902 Gr 2 Ti sheets, but electrode force has an insufficient effect. In contrast, of the 83.34% total parameter contribution, the welding current has the greatest impact (70.62%); the remaining portion is attributed to model error.
- NDT techniques, such as dye penetration testing and ultrasonic testing, did, however, verify that the nugget region generated during RSW did not have any compelling internal or exterior failures. It further demonstrated the importance of the proposed DoE runs and parameter settings for fabricating lap joints on AMS 4902 Gr 2 Ti sheets using RSW.
- In the meantime, when the weld current and welding cycle rise, so does the tensile load-carrying capacity. On

the other hand, while increasing electrode force from 2000N to 4000N, no appreciable changes were seen in the tensile load values of the proposed titanium sheet. However, after increasing the electrode force from 4000N to 6000N, the tensile load increased significantly to 7540N.

- The microstructure study shows a few needle-like features and alpha-structured grains resulting from the martensitic phase production and titanium annealing. Additionally, the microstructure's lack of twinning guaranteed the effectiveness of the examined electrode pressure range.
- The even distribution of hardness all over the weld nuggets in maximum and intermediate tensile strength specimens ensured the perfect welding among the interface.
- At last, the RSW process parameters were successfully optimized at 0.998942 desirability by the proposed complete factorial DoE. The study's ideal parameters were 10 kA of welding current, 40 cycles of welding duration, and 6000 N of electrode force, in that order. The confirmatory investigation demonstrated that the optimal tensile load of 8397.04N is extremely near to the real result attained at the optimal RSW process parameter setting of 8400N.

Hence, this study offers a practical recommendation of the proposed full factorial DoE method for optimizing RSW parameters to achieve superior weld quality and mechanical strength in thin titanium sheets. However, future research might analyze the effect of welding in other atmospheres, assess the long-term durability of welds subjected to cyclic loading and assess the adaptability of optimized parameters to other titanium grades and dissimilar metals. These studies will not only develop an understanding of RSW processes but also increase the applicability of findings across many engineering fields. While this study discusses tensile load testing, it is recognized that including additional mechanical tests such as fatigue resistance, hardness, and impact toughness would provide more understanding of weld quality. These tests will be considered for addition in future studies.

References

[1] Evren Atasoy, and Nizamettin Kahraman, "Diffusion Bonding of Commercially Pure Titanium to Low Carbon Steel Using a Silver Interlayer," *Materials Characterization*, vol. 59, no. 10, pp. 1481-1490, 2008. [Crossref] [Google Scholar] [Publisher Link]

[2] Hyoung-Keun Lee et al., "Optimization of Nd: YAG Laser Welding Parameters for Sealing Small Titanium Tube Ends," *Materials Science and Engineering: A*, vol. 415, no. 1-2, pp. 149-155, 2006. [Crossref] [Google Scholar] [Publisher Link]

[3] M. Katou et al., "Freeform Fabrication of Titanium Metal and Intermetallic Alloys by Three-Dimensional Micro Welding," *Materials & Design*, vol. 28, no. 7, pp. 2093-2098, 2007. [Crossref] [Google Scholar] [Publisher Link]

[4] Liu Liming et al., "Research on the Microstructure and Properties of Weld Repairs in TA15 Titanium Alloy," *Materials Science and Engineering: A*, vol. 445-446, pp. 691-696, 2007. [Crossref] [Google Scholar] [Publisher Link]

[5] Cui Chunxiang et al., "Titanium Alloy Production Technology, Market Prospects and Industry Development," *Materials & Design*, vol. 32, no. 3, pp. 1684-1691, 2011. [Crossref] [Google Scholar] [Publisher Link]

[6] M.S.F. Lima, F. Folio, and S. Mischler, "Microstructure and Surface Properties of Laser-Remelted Titanium Nitride Coatings on Titanium," *Surface and Coatings Technology*, vol. 199, no. 1, pp. 83-91, 2005. [Crossref] [Google Scholar] [Publisher Link]

[7] N. Saresh, M. Gopalakrishna Pillai, and Jose Mathew, "Investigations into the Effects of Electron Beam Welding on Thick Ti–6Al–4V Titanium Alloy," *Journal of Materials Processing Technology*, vol. 192-193, pp. 83-88, 2007. [Crossref] [Google Scholar] [Publisher Link]

[8] Tim Pasang et al., "Additive Manufacturing of Titanium Alloys–Enabling Re-Manufacturing of Aerospace and Biomedical Components," *Microelectronic Engineering*, vol. 270, 2023. [Crossref] [Google Scholar] [Publisher Link]

[9] T. Yokozeki et al., "Numerical Analysis of Impact and Postimpact Behavior of Titanium Matrix Composites for Landing Gear Application," *Proceedings of 16th European Conference of Composite Materials*, 2014. [Google Scholar]

[10] Yuji Marui, Toyotaka Kinoshita, and Kyo Takahashi, "47 Development of a Titanium Material by Utilizing Off-Grade Titanium Sponge," *SAE Technical Paper*, 2022. [Crossref] [Google Scholar] [Publisher Link]

[11] Nizamettin Kahraman, Behcet Gulenc, and Fehim Findik, "Corrosion and Mechanical-Microstructural Aspects of Dissimilar Joints of Ti–6Al–4V and Al plates," *International Journal of Impact Engineering*, vol. 34, no. 8, pp. 1423-1432, 2007. [Crossref] [Google Scholar] [Publisher Link]

[12] Z. Sun et al., "Effect of Laser Surface Remelting on the Corrosion Behavior of Commercially Pure Titanium Sheet," *Materials Science and Engineering: A*, vol. 345, no. 1-2, pp. 293-300, 2003. [Crossref] [Google Scholar] [Publisher Link]

[13] T.S. Balasubramanian et al., "Effect of Welding Processes on Joint Characteristics of Ti–6Al–4V Alloy," *Science and Technology of Welding and Joining*, vol. 16, no. 8, pp. 702-708, 2011. [Crossref] [Google Scholar] [Publisher Link]

[14] Y. Vahidshad, and A.H. Khodabakhshi, "An Investigation of Different Parameters on the Penetration Depth and Welding Width of Ti-6Al-4V Alloy by Plasma arc Welding," *Welding in the World*, vol. 65, no. 3, pp. 485-497, 2021. [Crossref] [Google Scholar] [Publisher Link]

[15] Shuwan Cui et al., "Microstructure, Texture, and Mechanical Properties of Ti-6Al-4V Joints by K-TIG Welding," *Journal of Manufacturing Processes*, vol. 37, pp. 418-424, 2019. [Crossref] [Google Scholar] [Publisher Link]

[16] Ali Gursel, "Crack Risk in Nd: YAG Laser Welding of Ti-6Al-4V Alloy," *Materials Letters*, vol. 197, pp. 233-235, 2017. [Crossref] [Google Scholar] [Publisher Link]

[17] J. Blackburn, "3-Laser Welding of Metals for Aerospace and Other Applications," *Welding and Joining of Aerospace Materials*, pp. 75-108, 2012. [Crossref] [Google Scholar] [Publisher Link]

[18] Marwan T. Mezher, Diego Carou, and Alejandro Pereira, "Exploring Resistance Spot Welding for Grade 2 Titanium Alloy: Experimental Investigation and Artificial Neural Network Modeling," *Metals*, vol. 14, no. 3, pp. 1-24, 2024. [Crossref] [Google Scholar] [Publisher Link]

[19] Dawei Zhao et al., "Research on the Correlation between Dynamic Resistance and Quality Estimation of Resistance Spot Welding," *Measurement*, vol. 168, 2021. [Crossref] [Google Scholar] [Publisher Link]

[20] T.E. Abioye et al., "Prediction of Tensile Shear Strength of Resistance Spot Welded AA 5052 Using Regression Analysis Model," *Materials Design and Applications III*, pp. 259-273, 2021. [Crossref] [Google Scholar] [Publisher Link]

[21] Dawei Zhao et al., "An Effective Quality Assessment Method for Small Scale Resistance Spot Welding Based on Process Parameters," *NDT & E International*, vol. 55, pp. 36-41, 2013. [Crossref] [Google Scholar] [Publisher Link]

[22] V. Zohoori-Shoar et al., "Resistance Spot Welding of Ultrafine Grained/Nanostructured Al 6061 Alloy Produced by Cryorolling Process and Evaluation of Weldment Properties," *Journal of Manufacturing Processes*, vol. 26, pp. 84-93, 2017. [Crossref] [Google Scholar] [Publisher Link]

[23] V.A. Klimenov et al., "Structure of Ti-6Al-4V Nanostructured Titanium Alloy Joint Obtained by Resistance Spot Welding," *AIP Conference Proceedings*, vol. 1698, no. 1, 2016. [Crossref] [Google Scholar] [Publisher Link]

[24] M. Shojaee et al., "Mechanical Properties and Failure Behavior of Resistance Spot Welded Third-Generation Advanced High Strength Steels," *Journal of Manufacturing Processes*, vol. 65, pp. 364-372, 2021. [Crossref] [Google Scholar] [Publisher Link]

[25] Nannan Chen et al., "Microstructural and Mechanical Evolution of Al/steel Interface with Fe_2Al_5 Growth in Resistance Spot Welding of Aluminum to Steel," *Journal of Manufacturing Processes*, vol. 34, pp. 424-434, 2018. [Crossref] [Google Scholar] [Publisher Link]

[26] Bikash Kumar et al., "A Comparative Study on Microstructural and Mechanical Behaviour of Spot Welded Ti-6Al-4V Alloy in as-welded and Solution Treated Condition," *Advances in Materials and Processing Technologies*, vol. 8, no. 3, pp. 2637-2651, 2022. [Crossref] [Google Scholar] [Publisher Link]

[27] Sumit K. Sharma et al., "Resistance Spot Welding of Aluminum 6063 Alloy for Aerospace Application: Improvement of Microstructural and Mechanical Properties," *Journal of the Institution of Engineers (India): Series D*, vol. 103, no. 1, pp. 311-318, 2022. [Crossref] [Google Scholar] [Publisher Link]

[28] Lihui Zhong et al., "Study on Influence of Electrode Type on Weld ability of TL091 Al. Alloy in Medium Frequency RSW," *Journal of Physics: Conference Series IOP Publishing*, vol. 2706, no. 1, pp. 1-9, 2024. [Crossref] [Google Scholar] [Publisher Link]

[29] Muhammad Safwan Mohd Mansor et al., "Microstructure and Mechanical Properties of Micro-Resistance Spot Welding between Stainless Steel 316L and Ti-6Al-4V," *The International Journal of Advanced Manufacturing Technology*, vol. 96, pp. 2567-2581, 2018. [Crossref] [Google Scholar] [Publisher Link]

[30] P. Bamberg et al., "Improvement of the Resistance Spot Welding of Al-Mg-Si Alloys by Using Cladding Technology: An Optical and Mechanical Characterization Study," *Journal of Advanced Joining Processes*, vol. 5, 2022. [Crossref] [Google Scholar] [Publisher Link]

[31] Aniruddha Ghosh, Somnath Chattopadhyaya, and Sergej Hloch, "Prediction of Weld Bead Parameters, Transient Temperature Distribution & HAZ Width of Submerged Arc Welded Structural Steel Plates," *Technical Journal*, vol. 19, no. 3, pp. 617-620, 2012. [Google Scholar] [Publisher Link]

[32] A.M. Pereira et al., "Effect of Process Parameters on the Strength of Resistance Spot Welds in 6082-T6 Aluminium Alloy," *Materials & Design (1980-2015)*, vol. 31, no. 5, pp. 2454-2463, 2010. [Crossref] [Google Scholar] [Publisher Link]

[33] Sergei Butsykin et al., "Effects of Preheating and Slow Cooling Stages in Small-Scale Resistance Spot Welding of the Ti-2Al-1Mn Alloy," *The International Journal of Advanced Manufacturing Technology*, vol. 128, no. 7-8, pp. 3011-3024, 2023. [Crossref] [Google Scholar] [Publisher Link]

[34] V.K. Prashanthkumar et al., "Process Parameter Selection for Resistance Spot Welding through Thermal Analysis of 2mm CRCA Sheets," *Procedia Materials Science*, vol. 5, pp. 369-378, 2014. [Crossref] [Google Scholar] [Publisher Link]

[35] Xiaobing Cao et al., "Modeling and Optimization of Resistance Spot Welded Aluminum to Al-Si Coated Boron Steel Using Response Surface Methodology and Genetic Algorithm," *Measurement*, vol. 171, 2021. [Crossref] [Google Scholar] [Publisher Link]

[36] M.R. Rawal et al., "Optimization of Resistance Spot Welding of 304 Steel Using GRA," *International Journal of Computer Engineering in Research Trends*, vol. 3, no. 9, pp. 492-499, 2016. [Crossref] [Google Scholar] [Publisher Link]

[37] Xiaodong Wan, Yuanxun Wang, and Dawei Zhao, "Multi-Response Optimization in Small Scale Resistance Spot Welding of Titanium Alloy by Principal Component Analysis and Genetic Algorithm," *The International Journal of Advanced Manufacturing Technology*, vol. 83, pp. 545-559, 2016. [Crossref] [Google Scholar] [Publisher Link]

[38] Tijana Rakić et al., "Comparison of Full Factorial Design, Central Composite Design, and Box-Behnken Design in Chromatographic Method Development for the Determination of Fluconazole and its Impurities," *Analytical Letters*, vol. 47, no. 8, pp. 1334-1347, 2014. [Crossref] [Google Scholar] [Publisher Link]

[39] Yakup Kaya, and Nizamettin Kahraman, "The Effects of Electrode Force, Welding Current and Welding Time on the Resistance Spot Weldability of Pure Titanium," *The International Journal of Advanced Manufacturing Technology*, vol. 60, pp. 127-134, 2012. [Crossref] [Google Scholar] [Publisher Link]

[40] T. Endramawan, and A. Sifa, "Non-Destructive Test Dye Penetrant and Ultrasonic on Welding SMAW Butt Joint with Acceptance Criteria ASME Standard," *IOP Conference Series: Materials Science and Engineering*, vol. 306, no. 1, pp. 1-9, 2018. [Crossref] [Google Scholar] [Publisher Link]

[41] J.R. Deepak et al., "Non-Destructive Testing, NDT Techniques for Low Carbon Steel Welded Joints: A Review and Experimental Study," *Materials Today: Proceedings*, vol. 44, pp. 3732-3737, 2021. [Crossref] [Google Scholar] [Publisher Link]

[42] Dawei Zhao et al., "Process Analysis and Optimization for Failure Energy of Spot Welded Titanium Alloy," *Materials & Design*, vol. 60, pp. 479-489, 2014. [Crossref] [Google Scholar] [Publisher Link]

[43] Sabah Khammass Hussein, and Osamah Sabah Barrak, "Analysis and Optimization of Resistance Spot Welding Parameter of Dissimilar Metals Mild Steel and Aluminum Using Design of Experiment Method," *Engineering and Technology Journal*, vol. 33, no. 8, pp. 1999-1011, 2015. [Google Scholar] [Publisher Link]

[44] Óscar Martín, Manuel López, and Fernando Martín, "Artificial Neural Networks for Quality Control by Ultrasonic Testing in Resistance Spot Welding," *Journal of Materials Processing Technology*, vol. 183, no. 2-3, pp. 226-233, 2007. [Crossref] [Google Scholar] [Publisher Link]

[45] Abbas Moghanizadeh, "Evaluation of the Physical Properties of Spot Welding Using Ultrasonic Testing," *The International Journal of Advanced Manufacturing Technology*, vol. 85, pp. 535-545, 2016. [Crossref] [Google Scholar] [Publisher Link]

[46] Xu Guirong et al., "Analysis and Innovation for Penetrant Testing for Airplane Parts," *Procedia Engineering*, vol. 99, pp. 1438-1442, 2015. [Crossref] [Google Scholar] [Publisher Link]

[47] Regita Bendikiene et al., "Comparative Study of TIG Welded Commercially Pure Titanium," *Journal of Manufacturing Processes*, vol. 36, pp. 155-163, 2018. [Crossref] [Google Scholar] [Publisher Link]

[48] Yuri Shchitsyn et al., "Formation of Structure and Properties of Two-Phase Ti-6Al-4V Alloy during Cold Metal Transfer Additive Deposition with Interpass Forging," *Materials*, vol. 14, no. 16, pp. 1-18, 2021. [Crossref] [Google Scholar] [Publisher Link]

[49] Nizamettin Kahraman, "The Influence of Welding Parameters on the Joint Strength of Resistance Spot-Welded Titanium Sheets," *Materials & Design*, vol. 28, no. 2, pp. 420-427, 2007. [Crossref] [Google Scholar] [Publisher Link]

[50] P. Rajalingam et al., "Ultrasonic Spot-Welding of AA 6061-T6 Aluminium Alloy: Optimization of Process Parameters, Microstructural Characteristics and Mechanical Properties of Spot Joints," *International Journal of Lightweight Materials and Manufacture*, vol. 7, no. 1, pp. 25-36, 2024. [Crossref] [Google Scholar] [Publisher Link]

[51] Dawei Zhao et al., "Multi-Objective Optimization of the Resistance Spot Welding Process Using a Hybrid Approach," *Journal of Intelligent Manufacturing*, vol. 32, pp. 2219-2234, 2021. [Crossref] [Google Scholar] [Publisher Link]

[52] Dawei Zhao et al., "Welding Quality Evaluation of Resistance Spot Welding Based on a Hybrid Approach," *Journal of Intelligent Manufacturing*, vol. 32, no. 7, pp. 1819-1832, 2021. [Crossref] [Google Scholar] [Publisher Link]

[53] Marwan T. Mezher, Diego Carou, and Alejandro Pereira, "Exploring Resistance Spot Welding for Grade 2 Titanium Alloy: Experimental Investigation and Artificial Neural Network Modelling," *Metals*, vol. 14, no. 3, pp. 1-24, 2024. [Crossref] [Google Scholar] [Publisher Link]

[54] Sudhakar Uppada et al., "Optimization of Process Parameters in Resistance Spot Welding Using Artificial Immune Algorithm," *Innovative Product Design and Intelligent Manufacturing Systems: Select Proceedings of ICIPDIMS 2019*, pp. 477-485, 2020. [Crossref] [Google Scholar] [Publisher Link]

[55] Fatih Bozkurt et al., "The Effect of Welding Parameters on Static and Dynamic Behaviors of Spot Welded Ti6AL4V Sheets," *Journal of Materials Engineering and Performance*, vol. 29, pp. 7468-7479, 2020. [Crossref] [Google Scholar] [Publisher Link]

[56] Iqbal Taufiqurrahman et al., "The Effect of Welding Current And Electrode Force on the Heat Input, Weld Diameter, and Physical and Mechanical Properties of SS316l/Ti6Al4V Dissimilar Resistance Spot Welding with Aluminum Interlayer," *Materials*, vol. 14, no. 5, pp. 1-20, 2021. [Crossref] [Google Scholar] [Publisher Link]